ELSEVIER

Chemical Geology 195 (2003) 69–85

CHEMICAL GEOLOGY
INCLUDING
ISOTOPE GEOSCIENCE

www.elsevier.com/locate/chemgeo

Nonbiological fractionation of Fe isotopes: evidence of an equilibrium isotope effect

J.E. Roe[a], A.D. Anbar[a,b,*], J. Barling[b]

[a] *Department of Chemistry, University of Rochester, Rochester, NY 14627, USA*
[b] *Department of Earth and Environmental Sciences, University of Rochester, Rochester, NY 14627, USA*

Received 1 April 2001; received in revised form 3 January 2002

Abstract

Fe isotopes can be fractionated to similar extent by both biological and nonbiological processes in the laboratory. However, fractionation mechanisms are not yet clear, making it difficult to generalize from the laboratory to natural systems. We have previously shown that Fe isotope fractionations of several per mil can be generated during anion exchange chromatography of Fe dissolved in HCl. Here, we present results of experiments designed to assess the importance of equilibrium Fe isotope effects in such systems. In batch equilibration rate experiments, including one using a ^{54}Fe-enriched tracer to precisely determine the rate of exchange between dissolved and resin-bound Fe, equilibration was nearly complete within 1 min. In rate-dependent chromatographic elution experiments, the extent of isotope separation was found to increase significantly as flow rate decreased, demonstrating that the magnitude of Fe isotope fractionation increases as more time is allowed for equilibration. This observation provides very strong evidence of a significant equilibrium isotope effect, while also revealing that expression of this effect can be inhibited if the flow rate is higher than the time constant for equilibration. We propose that diffusion into resin pores is the rate-limiting step inhibiting complete expression of equilibrium isotope fractionation. Fractionation of Fe isotopes in this system most likely reflects an equilibrium effect during speciation between Fe chloro–aquo complexes, particularly between anionic, tetrahedral $FeCl_4^-$ and the sixfold coordinated $FeCl_3(H_2O)_3^0$ and $FeCl_2(H_2O)_4^+$. On theoretical grounds, such changes in bonding environment are likely to drive Fe isotope fractionation. The magnitude of the equilibrium fractionation factor is likely 1.0001 to 1.001. Extrapolating from these results, Fe isotope variations in nature cannot be uniquely ascribed to biology until nonbiological Fe isotope effects are better understood.

Keywords: Fe; Isotope composition; Mass fractionation; Anion exchange chromatography

1. Introduction

Precise measurements of mass-dependent variations in the isotopic compositions of elements heavier than sulfur have been greatly facilitated by the development of multiple collector inductively coupled plasma mass spectrometry (MC-ICP-MS) (Walder

* Corresponding author. Department of Earthland Environmental Sciences, University of Rochester, Rochester, NY 14627, USA. Tel.: +1-585-275-5923; fax: +1-585-244-5689.
E-mail address: anbar@earth.rochester.edu (A.D. Anbar).

0009-2541/02/$ - see front matter © 2002 Elsevier Science B.V. All rights reserved.
doi:10.1016/S0009-2541(02)00389-3

and Freedman, 1992; Walder et al., 1993; Halliday et al., 1995). This new technology has stimulated research into isotope fractionations of transition metals (e.g., Cu, Zn, Mo, Tl and Fe) in nature and in the laboratory (Maréchal et al., 1999; Anbar et al., 2000; Rehkamper and Halliday, 1999; Zhu et al., 2000a,b). Study of the stable isotope biogeochemistry of transition metals is expected to provide insights into the processing of these elements in the environment and in biology.

Iron is of special interest because it is abundant at the Earth's surface, and because its use in biology is ubiquitous. The possibility that the Fe isotopic composition of ancient sediments can be used as a biosignature has motivated much recent work (Beard et al., 1999; Anbar et al., 2000; Zhu et al., 2000a,b; Bullen et al., in press; Brantley et al., in press). This application is based on the observation that δ^{56}Fe (=[(^{56}Fe/^{54}Fe)$_{\mathrm{Sample}}$/(^{56}Fe/^{54}Fe)$_{\mathrm{Standard}}-1]\times 1000‰$) of dissolved Fe(II) is shifted by $\sim -1‰$ during microbially mediated reduction of ferrihydrite in the laboratory (Beard et al., 1999).

The discovery that nonbiological chemical processes can also fractionate Fe isotopes is a potential complication for biosignature applications of the Fe isotope system (Anbar et al., 2000; Bullen et al., in press). Anbar et al. (2000) reported fractionation of $\sim 7‰$ during elution of Fe in 2 M HCl from an anion exchange column. Isotope fractionation during ion exchange is well known for a number of other elements, including Li, (Taylor and Urey, 1938), B (Kakihana et al., 1977), Ca (Russell et al., 1978), Ga (Machlan and Gramlich, 1988) and Cu (Maréchal et al., 1999) but had not previously been demonstrated for Fe. Subsequently, Bullen et al. (in press) reported fractionation on the order of 1‰ during oxidation and precipitation of ferrihydrite from dissolved Fe(II). These findings suggest that nonbiological processes may contribute to δ^{56}Fe variations in sediments. However, until natural δ^{56}Fe variations of unambiguous nonbiological origin are observed, generalization from laboratory experiments requires some understanding of the fractionation mechanism.

Significantly, both Anbar et al. (2000) and Bullen et al. (in press) found that the reaction products were isotopically heavier than the starting materials: in ion exchange experiments, δ^{56}Fe in the earliest eluate was >0; in precipitation experiments, δ^{56}Fe of the precipitate was >0. These findings are not consistent with simple kinetic effects, which should yield products isotopically lighter than reactants. As a result, the authors of both studies proposed that their observations indicated the existence of equilibrium isotope effects between dissolved Fe species. To explain the ion exchange results, it was proposed that lighter Fe isotopes preferentially partition into the anionic $FeCl_4^-$ complex which adsorbs to the anion exchange resin, while heavier isotopes preferentially partition into cationic or neutral Fe species that do not adsorb (i.e., $Fe(H_2O)_6^{3+}$, $FeCl(H_2O)_5^{2+}$, $FeCl_2(H_2O)_4^+$, $FeCl_3(H_2O)_3^\circ$). Similarly, the ferrihydrite results were explained in terms of preferential partitioning of heavy Fe isotopes into the most rapidly oxidized species, $Fe(OH)(H_2O)_5^+$ and $Fe(OH_2)(H_2O)_4^\circ$.

Because of the complicated speciation of Fe in nature, and the frequent separation of Fe species based on their differing solubilities or reactivities, it has been predicted that isotopic variations in nature should be widespread, and need not reflect only biological processing of Fe (Anbar et al., 2000; Bullen et al., in press). In the case of ion exchange columns, this interpretation was challenged by Skulan et al. (2000) and Beard et al. (2000). These authors explained the observed fractionation in terms of "transient" phenomena related to kinetic isotope effects specific to the ion exchange column.

Here, we report the results of four experiments designed to test the hypothesis that equilibrium isotope effects underlie the fractionation of Fe isotopes during anion exchange chromatography. These include two batch equilibration experiments between dissolved and resin-bound Fe, as well as two chromatographic experiments. The first batch experiment investigated the extent and variation of Fe isotope fractionation during a single-step equilibration between Fe(III) in HCl and Biorad AG MP-1 resin over 24 h. This experiment was intended to provide gross constraints on the magnitude of equilibrium fractionation and on the rate of equilibration. In a second batch experiment, a ^{54}Fe-enriched spike was used to precisely measure the rate of equilibration. The two chromatographic experiments were designed so that all elution parameters were identical

except for the flow rates during elution, which differed by a factor of 10. Differences in the extent of fractionation between these two experiments can be used to assess the importance of kinetic factors during elution.

2. Background

2.1. Ion exchange separation

Ion exchange chromatography can be used to separate individual elements of a sample. In ICP-MS, sample purification is necessary to avoid isobaric interferences or matrix effects from other elements, which could lead to errors in sample analysis. Erroneous results could also be produced if the separation process itself causes isotopic fractionation. Consequently, it is necessary to determine the extent of fractionation during ion exchange.

Ion exchange separations are based on the equilibration of one or more species of the element of interest between two phases—a stationary phase (ion exchanger) and a mobile phase (solution). Because the chemical speciation in the mobile phase is usually not well known, the partitioning of an element between these phases is usually described in terms of an equilibrium distribution coefficient (K_D). $K_D = C_r/C_s$, where C_r is the total concentration of the element on the resin, and C_s the total concentration in solution (Harris, 1991; Skoog and Leary, 1992).

Separations of two or more elements can be achieved if their K_D values differ by separating the solution from the resin following a single batch equilibration between a solution containing a mixture of the elements and the resin. In the case of elements A and B, with an initial concentration ratio of ${}^{A}C_i/{}^{B}C_i$ and distribution coefficients ${}^{A}K_D$ and ${}^{B}K_D$, the ratio of their concentrations in the resin-equilibrated solution, ${}^{A}C_s/{}^{B}C_s$, is equal to ${}^{A}C_i/{}^{B}C_i \times (V_s + V_r{}^{B}K_D)/(V_s + V_r{}^{A}K_D)$. Here, V_s and V_r are the volumes of solution and resin, respectively. It is apparent that ${}^{A}C_s/{}^{B}C_s > {}^{A}C_i/{}^{B}C_i$ if ${}^{B}K_D/{}^{A}K_D > 1$, and that ${}^{A}C_s/{}^{B}C_s \sim {}^{A}C_i/{}^{B}C_i \times {}^{B}K_D/{}^{A}K_D$ when the K_D values are large.

A much more efficient "chromatographic" separation can be accomplished by passing the mixed solution through a column packed with ion exchanger. In this case, the rate at which the elements migrate through the column will correlate inversely with their K_D values. The advantage of this process is classically visualized by considering the column as a series of "theoretical plates", in which each plate is the equivalent of one batch extraction (Martin and Synge, 1941; Gluekauf, 1955; Skoog and Leary, 1992). Typically the number of plates in a column range from 50 to >1000 depending on column parameters (e.g., length and diameter of the column and flow rate through the column) and the type and concentration of the eluate. As the solution flows from each plate to the next, the concentrations in solution and on the resin adjust toward a "local" equilibrium between the two phases. In an ideal column, this "local" equilibrium will be attained at each plate before the solution passes to the next plate. This results in the maximum separation between the elements. In the extreme case of the earliest, infinitesimal drop of eluate, ${}^{A}C_s/{}^{B}C_s = {}^{A}C_i/{}^{B}C_i \times [(V_s + V_r{}^{B}K_D)/(V_s + V_r{}^{A}K_D)]^n$ where n is the number of plates. Hence, even a small difference between ${}^{B}K_D$ and ${}^{A}K_D$ may be amplified by column chromatography.

A rigorous mathematical description of the expected concentration in each elution fraction can be found in Martin and Synge (1941). In the ideal case, the concentration of each element in the elution fractions describes a symmetric, Gaussian distribution. In practice, complete local equilibrium is often not achieved, resulting in an asymmetric elution curve. Column parameters such as particle size of the resin, length of the column and flow rate can be optimized to produce near-equilibrium conditions (Helfferich, 1995).

The stationary phase in our experiments, and in the experiments of Anbar et al. (2000), is AG MP-1 resin (Biorad). This is a strongly basic anion exchange resin with positively charged quaternary ammonium functional groups ($[R\text{-}CH_2N(CH_3)_3]^+$) bound to a styrene divinyl benzene backbone (Marhol, 1982). Significantly, AG MP-1 is a so-called "macroporous" resin; the resin beads are perforated with large pores (M.W. exclusion $>10^6$), which contain the functional groups at their surface, making these sites more accessible. This resin also has micropores (M.W. exclusion $\sim 10^3$) typical of the anion and cation resins commonly used in geochemical applications. Van der Walt et al. (1985) has shown improved

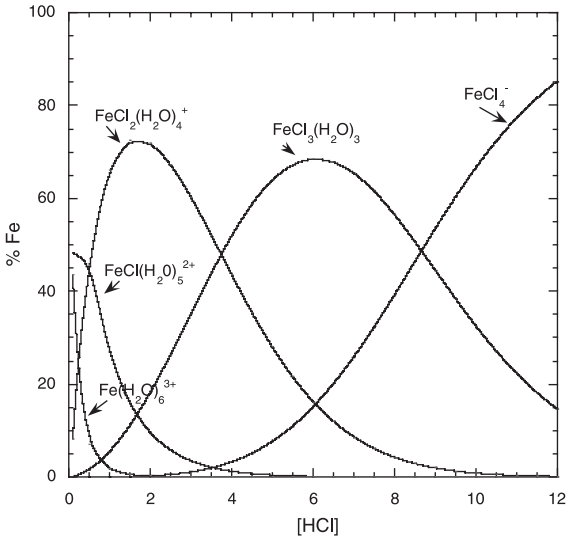

Fig. 1. Distribution of Fe chloro–aquo species as a function of [HCl]. In calculations of Fe speciation, which use Cl^- activity (a_{Cl^-}), a_{Cl^-} is related to [Cl^-] using the equation $\log a_{Cl^-} = -0.45 + 0.187 \times [HCl]$ (Bjerrum et al., 1986). It should be noted that these calculations do not include the reaction $FeCl_4^- + R\text{-}Cl$. The presumably large equilibrium constant for this reaction should shift the speciation toward the anionic complex upon exposure to the resin.

equilibration kinetics for the AG MP-1 resin over microporous AG1 × 8 for inorganic complexes of Fe and other transition metals as demonstrated by an observed decrease in tailing during elution with the AG MP-1. Consequently there is also an improved separation.

Because it is not a true equilibrium constant, the value of K_D may vary with solution composition. Of particular importance here, the K_D for Fe(III) on anion exchange resin increases with the activity of Cl^- (a_{Cl^-}). This phenomenon can be understood qualitatively in terms of the speciation of Fe(III) in HCl media, which is dominated by the complexes $Fe(H_2O)_6^{3+}$, $FeCl(H_2O)_5^{2+}$, $FeCl_2(H_2O)_4^+$, $FeCl_3(H_2O)_3^\circ$ and $FeCl_4^-$ (Bjerrum and Lukes, 1986). These complexes are believed to equilibrate relatively rapidly on laboratory timescales (Strahm et al., 1979; Connick and Coppel, 1959; Schwarz and Dodson, 1976).

$FeCl_4^-$ is the only anionic form of Fe(III), and adsorbs to the resin by displacing the Cl^- counterion: $FeCl_4^- + R\text{-}Cl \rightleftharpoons R\text{-}FeCl_4 + Cl^-$. Because an increase in a_{Cl^-} shifts the equilibrium speciation toward $FeCl_4^-$ (Fig. 1; Table 1), the magnitude of K_D and a_{Cl^-} are positively correlated (Table 2). This trend is countered by the tendency of Cl^- to displace $FeCl_4^-$ from the exchange sites on the resin as a_{Cl^-} increases. However, this displacement effect does not dominate under the conditions studied here. Therefore, in the experiments described below, and in Anbar et al. (2000), Fe is typically "loaded" onto the ion exchanger in ~7 M HCl, and eluted in =2 M HCl.

2.2. Previous observations and hypotheses

Fractionation of Fe isotopes during elution from an ion exchange column has been reported previously (Fig. 2; Anbar et al., 2000). In these experiments, Fe was dissolved in 1 ml of 7 M HCl + 0.001% H_2O_2 and loaded onto ~2 cm^3 of AG MP-1 resin packed in a polypropylene column (0.5 $cm^2 \times 3.7$ cm). The Fe was eluted using ~8 ml of 2 M HCl + 0.001% H_2O_2. The earliest elution fractions were found to be enriched in the heavier isotope ($\delta^{56}Fe > 0$) compared to the loaded Fe ($\delta^{56}Fe = 0$), while the last fractions were depleted ($\delta^{56}Fe < 0$). The $\delta^{56}Fe$ values over the entire elution curve ranged from 3.6‰ to −3.4‰.

We proposed that the observed fractionation of Fe isotopes occurred as the result of an equilibrium isotope fractionation during one or more of reactions 1–5 (Table 1) such that the relative abundance of the heavier isotope is enriched in solution. Equilibrium isotope effects arise from differences in free energies of the equilibrating species, and result in the redistribution of the isotopes such that heavier isotopes are preferentially partitioned into the stronger bonding environments (Hoefs, 1989; Criss, 1999). For exam-

Table 1
Equilibrium reactions of Fe(III)–chloro complexes and their stability constants

(1) $Fe(H_2O)_6^{3+} + Cl^- \rightleftharpoons FeCl(H_2O)_5^{2+}$	K_1=30
(2) $FeCl(H_2O)_5^{2+} + Cl^- \rightleftharpoons FeCl_2(H_2O)_4^+$	K_2=4.5
(3) $FeCl_2(H_2O)_4^+ + Cl^- \rightleftharpoons FeCl_3(H_2O)_3^\circ$	K_3=0.15
(4) $FeCl_3(H_2O)_3^\circ + Cl^- \rightleftharpoons FeCl_4^-$	K_4=0.0078
(5) $FeCl_4^- + R\text{-}Cl \rightleftharpoons R\text{-}FeCl_4 + Cl^-$	K_R

Equilibrium constants from Bjerrum and Lukes (1986).

Table 2
K_D of Fe^{3+} on AG MP-1 resin in HCl

[HCl] (M)	K_D
7	1390[a]
5	158[a]
3	19.6[a]
2	6.6[b]

[a] Van der Walt et al. (1985).
[b] This study.

ple, reaction 4 can be written independently for the two major isotopes of Fe:

$$^{54}FeCl_3(H_2O)_3^\circ + Cl^- \leftrightarrow {}^{54}FeCl_4^- + 3H_2O \quad {}^{54}K_4$$

$$^{56}FeCl_3(H_2O)_3^\circ + Cl^- \leftrightarrow {}^{56}FeCl_4^- + 3H_2O \quad {}^{56}K_4$$

If $^{54}K_4 \neq {}^{56}K_4$, then it is straightforward that $([^{56}FeCl_4^-]/[^{56}FeCl_3(H_2O)_3^\circ]) \times ([^{54}FeCl_3(H_2O)_3^\circ]/[^{54}FeCl_4^-]) = ([^{56}FeCl_4^-]/[^{54}FeCl_4^-]) \times ([^{54}FeCl_3(H_2O)_3^\circ]/[^{56}FeCl_3(H_2O)_3^\circ]) = (^{56}Fe/^{54}Fe)_{FeCl_4^-}/(^{56}Fe/^{54}Fe)_{FeCl_3(H_2O)_3^\circ} = {}^{56}K_4/{}^{54}K_4 \neq 1$. Hence, the isotopic composition of Fe will be different in the anionic and neutral species, resulting in a difference in isotopic composition between Fe in the mobile and stationary phases. This mass-dependent difference in equilibrium constants translates directly into a difference in K_D between the isotopes. This difference is analogous to that between chemical species; $^{56}K_D$ and $^{54}K_D$ replace $^{A}K_D$ and $^{B}K_D$ in the previous expressions (Section 2.1). Hence, in a batch experiment, $[^{56}Fe]_s/[^{54}Fe]_s = [^{56}Fe]_r/[^{56}Fe]_r \times {}^{54}K_D/{}^{56}K_D = [^{56}Fe]_i/[^{54}Fe]_i \times (V_s + V_r^{54}K_D)/(V_s + V_r^{56}K_D)$. $^{54}K_D/^{56}K_D$ can be estimated from chromatographic data by plotting the isotopic composition of each elution fraction against cumulative %Fe eluted on a probability abscissa (Gluekauf, 1958; Russell and Papanastassiou, 1978). Using this approach, Anbar et al. (2000) derived an order-of-magnitude estimate of $^{54}K_D/^{56}K_D \sim 1.0001$. This small effect is amplified by the chromatography column to produce isotope fractionation in the range 1–10‰ during elution.

The preceding treatment assumes that local equilibrium is maintained during elution. However, Fig. 2 shows evidence of nonideal behavior during elution of Fe, in the form of an extended elution tail. This indicates that local equilibrium has not been *fully* achieved, which raises the possibility that kinetic isotope effects may influence the observed isotope fractionation. Kinetic isotope effects arise from mass-dependent differences in reaction rates, and can be manifested by incomplete or unidirectional processes (Hoefs, 1989). Chemical reactions such as 1–5 (Table 1) probably equilibrate rapidly on the timescale of our experiments. Therefore, nonideal behavior most likely results from incomplete physical processes, such as diffusion of Fe complexes through the resin structure. If the diffusion timescale is slow relative to the elution flow rate, then complete equilibration between dissolved and resin-bound Fe cannot be achieved at each plate as the solution travels down the column. Essentially, diffusion becomes the rate-limiting step in the equilibration of dissolved and resin-bound Fe. Diffusive artifacts are well known in chromatography (Helfferich, 1995).

Such effects could substantially influence the observed isotope fractionation. Whether this influence leads to a larger or smaller isotope fractionation than would be observed at equilibrium depends on the mass dependence of the rate-limiting step (in the case of diffusion, this means the mass dependence of diffusion coefficients). At one extreme, it is possible that the mass discrimination during the rate-limiting process is very large compared to any equilibrium

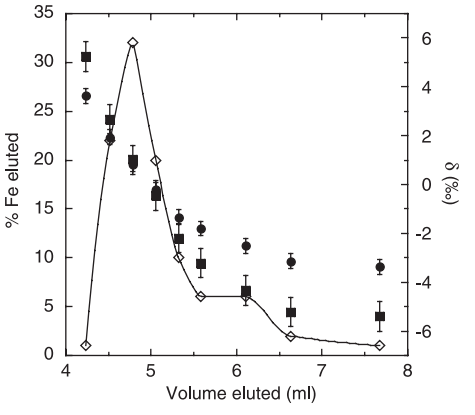

Fig. 2. Fe elution curve and Fe isotopic compositions for typical anion exchange chromatographic experiment (Anbar et al., 2000). $\delta^{56}Fe$ and $\delta^{57}Fe$ of the Fe loaded on the column = 0. Fe was eluted in 2 M HCl. $\delta^{56}Fe$ (●) and $\delta^{57}Fe$ (■) from the fractions of Fe collected during elution are shown. The early fractions collected show $\delta Fe > 0$ while the later fractions show that $\delta Fe < 0$ ~ 100% of the Fe loaded to the column was recovered. When integrated over all elution fractions, $\delta^{56}Fe \sim 0$ as required by mass balance.

isotope effects. In this case, the hypothesis outlined above is invalidated; equilibrium effects would be trivial or nonexistent and the observed isotope fractionation would originate in kinetic isotope effects specific to the ion exchange system. At the other extreme, it is possible that there is little or no mass discrimination during the rate-limiting process, so that the equilibrium hypothesis is valid in general, if not in exact detail. Lack of complete equilibration could then result in a *smaller* isotope effect than would be observed if complete equilibration were achieved.

Intermediate scenarios are also possible, in which both equilibrium and kinetic isotope effects contribute to the observed isotope fractionation. These effects could combine to produce an overall fractionation either larger or smaller than in the ideal case, depending on the reaction details. The experiments described here are designed to provide insight into which of these alternatives apply to this system.

3. Experimental design

3.1. Equilibration rate experiments

The asymmetry of the elution curve in Fig. 2 provides only a crude indication of disequilibrium during elution. To more rigorously constrain the rate of equilibration between dissolved and resin-bound Fe, two batch experiments were conducted.

In experiment #1, Fe was first "loaded" onto resin by equilibration in 7 M HCl + 0.001% H_2O_2 (K_D ~1400) (Van der Walt et al., 1985) and then desorbed by lowering [HCl] to ~2 M HCl + 0.001% H_2O_2 (K_D ~ 6). The isotopic composition and concentration of dissolved Fe in the solution was then measured at intervals over a 24-h period. The isotopic composition of resin-bound Fe was also measured after 24 h for comparison. This experiment was designed to provide a rough constraint on the rate of equilibration, and to check for consistency with the prediction that $^{54}K_D/^{56}K_D$ is of order 1.0001 (Anbar et al., 2000).

In experiment #2, an ^{54}Fe-enriched tracer (δ^{56}Fe = − 998 ‰) was loaded onto resin by equilibration in 2 M HCl + 0.001% H_2O_2 for 24 h. The equilibrated solution was then decanted and replaced with another 2 M HCl + 0.001% H_2O_2 solution containing the same volume and concentration of isotopically normal Fe (δ^{56}Fe = 0 ‰). δ^{56}Fe of dissolved Fe was then followed for 12 h. The isotopic composition of resin-bound Fe was measured after 12 h for comparison. Because of the extreme isotopic contrast between the tracer and normal Fe, and the precision of our analytical methods, this experiment allows us to place a tight constraint on the equilibration rate.

3.2. Rate dependence experiments

Equilibration rate experiments provide no information on whether or not the rate-limiting step is mass-dependent. Therefore, demonstration of incomplete equilibration is not, on its own, sufficient to invalidate the equilibrium fractionation hypothesis. To directly address this issue, we conducted two chromatographic experiments at vastly different flow rates. The experiments were otherwise identical: Fe was "loaded" on an ion exchange column in 7 M HCl + 0.001% H_2O_2, and eluted in 2 M HCl + 0.001% H_2O_2 in a series of elution fractions. The Fe concentration and isotopic compositions were analyzed in each fraction.

There are only three possible outcomes of these experiments, each with mechanistic implications:

(a) Isotope fractionation could be found to be *independent* of flow rate. This would demonstrate that kinetic effects are unimportant.
(b) Isotope fractionation could be found to *decrease* at the slower flow rate. Because slower flow leads to more complete equilibration as the solution spends more time in contact with the resin at each "theoretical plate", this finding would demonstrate that the fractionation magnitude decreases as equilibrium is approached. Hence, this would be evidence that the observed fractionation is caused by a kinetic isotope effect during the rate-limiting step. This finding would not preclude existence of an equilibrium isotope effect, but would permit the possibility that such an effect is trivially small.
(c) Isotope fractionation could be found to *increase* at the slower flow rate. In contrast to (b), this finding would demonstrate that the fractionation magnitude increases as equilibrium is approached. Hence, this would provide strong evidence of a significant equilibrium isotope effect.

4. Materials, experimental details and analytical methods

4.1. Materials

All experiments described here were carried out in a positively pressurized metal-free clean lab with a HEPA-filtered air supply. Plastics and glassware were pre-cleaned. Polypropylene centrifuge tubes and clear plastic pipette tips were acid-cleaned in 6 M HCl for a minimum of 1 week prior to use, rinsed with 18 M-Ohm deionized (DI) H_2O and allowed to dry in a laminar air hood. HDPE plastics, glass and polypropylene columns were acid-cleaned in a 20% HNO_3 acid bath for 1 week, rinsed with 18 M-Ohm DI H_2O, followed by cleaning in a 20% HCl bath for 1 week and another 18 M-Ohm DI H_2O rinse. Teflon PFA screw-top beakers (Savillex) and FEP (Nalgene) bottles were soaked in 1% Micronox soap diluted with DI H_2O and then cleaned for a minimum of 24 h in hot 50% HNO_3, then a minimum of 24 h in hot 50% HCl, followed by a final step of 24 h in hot 18 M-Ohm DI H_2O. Between each step and at the end, beakers were thoroughly rinsed with 18 M-Ohm DI H_2O.

The acids in the experiments and was for dilution of samples and standards were ultrapure sub-boiling quartz-distilled HCl or HNO_3 acids (Seastar Baseline). High purity H_2O_2 (JT Baker, Ultrex) was used in the procedures. This was added to the eluate in small amounts to inhibit the reduction of Fe(III) to Fe(II) by the resin. Both the acids and H_2O_2 were diluted, as required, using 18 M-Ohm DI H_2O.

Before use, the resin (Biorad AG MP-1, 100–200 mesh, Cl^- form) was cleaned of Cu, Fe, Mn and Zn using 3 column volumes of 0.5 M HNO_3 followed by 1 column volume of 18 M-Ohm H_2O. This procedure was repeated twice, after which the resin was conditioned with 2 column volumes of the either 2 or 7 M HCl + 0.001% H_2O_2, depending on the experiment.

The Fe used for this investigation (Johnson–Matthey Specpure ICP Fe Lot #8025868; "JMC-Fe") was reduced almost to dryness and redissolved in either 2 or 7 M HCl for experiments. For isotope ratio measurements, JMC-Fe was used as our in-house Fe isotope standard ($\delta^{56}Fe_{JMC\text{-}Fe} \equiv 0$ ‰). The standard and samples were doped with Cu (Johnson–Matthey Specpure ICP Cu, Lot #702499H; "JMC-Cu") standard solution reconstituted in 0.05 M HNO_3. The JMC-Fe standard was stored in acid-cleaned HDPE bottles at concentrations of 3 or 4 ppm, while the JMC-Cu was stored in acid-cleaned Teflon bottles at a concentration of 100 ppm.

A ^{54}Fe-enriched tracer was used in the equilibration rate experiments and in the preparation of a gravimetric standard for quality control in MC-ICP-MS analysis. ^{54}Fe-enriched Fe metal (97.7% ^{54}Fe) was purchased from Oak Ridge National Laboratory. This metal was dissolved in concentrated HNO_3. The Fe concentration was determined using reverse isotope dilution by MC-ICP-MS. The isotopic composition of this solution was also characterized by MC-ICP-MS.

For quality-control purposes, a ^{54}Fe-enriched standard was prepared by addition of a known amount of the ^{54}Fe tracer to a known amount of the JMC-Fe standard, thus changing the isotopic composition of the standard by a known amount. All quantities were determined by careful gravimetry. δ^{56}Fe of this "Grav-Fe" standard was -10.9 ‰.

4.2. Equilibration rate experiments

The equilibration rate batch experiments were designed so that each aliquot of the acid solution contained sufficient Fe for a precise measurement of Fe isotope ratios (minimum of 4 μg) and for determination of the Fe concentration (minimum of 3 μg). Because K_D vs. [HCl] is known (Table 2), the amount of Fe on the resin and in the solution can be calculated. This also allows for the volume of resin and acid to be optimized to produce the desired Fe concentration of the acid solution.

In experiment #1, 1000 μg of JMC-Fe standard in ~ 6 ml of 7 M HCl + 0.001% H_2O_2 was added to 8 cm^3 of wet resin (previously conditioned with 7 M HCl + 0.001% H_2O_2). The resin–solution mixture was shaken with a mechanized shaker for 4 h. Once the resin and solution had been mixed, the mixture was allowed to stand for 48 h to ensure complete equilibration.

A final HCl concentration of 1.6 M in the solution was achieved by the addition of ~ 27 ml of 18 M-Ohm DI H_2O to the resin–solution mixture. The mixture was shaken for 4 h, during which time solution aliquots were taken at timed intervals using a 10 ml polypropylene syringe equipped with a 0.2 μm syringe filter.

The solutions were transferred to centrifuge tubes and saved for analysis.

In experiment #2, 10 ml of a 49 ppm ^{54}Fe-enriched tracer solution in 2 M HCl + 0.001% H_2O_2 was added to 2 cm^3 of wet resin. The mixture was shaken with a mechanized shaker for 4 h. Once the resin and solution had been mixed, the mixture was allowed to stand for 48 h to ensure complete equilibration. The solution was then separated from the resin by centrifugation. The Fe concentration of the extracted spike solution was 40 ppm as determined by UV–VIS spectrophotometry, within error of the expected concentration of 37 ppm predicted from known K_D (Table 2).

This resin, loaded with ^{54}Fe-enriched Fe, was then mixed with 10 ml of 2 M HCl + 0.001% H_2O_2, containing 40 ppm of JMC-Fe standard. The mixture was shaken for 4 h, during which time solution aliquots were taken at timed intervals using a 10-ml polypropylene syringe equipped with a 0.2-μm syringe filter. The solutions were transferred to centrifuge tubes and saved for analysis.

In both experiments, after the last aliquot was taken the remaining resin and solution were separated by vacuum filtration. Ten milliliters of 0.5 M HCl + 0.001% H_2O_2 was used to disaggregate the resin cake and transfer the resin to a polypropylene column. This solution was saved. An additional 10 ml of 0.5 M HCl + 0.001% H_2O_2 was passed through the resin to ensure that all of the Fe had eluted from the resin, and added to the saved solution. The entire 20 ml of 0.5 M HCl + 0.001% H_2O_2 was collected in a single Teflon beaker for subsequent determination of the quantity and isotopic composition of resin-bound Fe. The amount of Fe in the timed aliquots and remaining on the resin was determined by UV–VIS analysis.

4.3. Rate dependence experiments

Two column chromatography experiments were performed which were identical except for the flow rate through the column during elution. The flow rate was accelerated for the "fast" column by pressurization using a peristaltic pump. The pump was attached to the funnel at the top of the column to produce a controlled flow rate of 50–60 drops/min (~3 ml/min). For the "slow" column, a stopcock was used to decrease the flow rate to 5–6 drops/min (~0.3 ml/min).

Both experiments utilized a glass column (0.7 cm diameter) containing 2.2 cm^3 of resin. JMC-Fe standard (2100 μg) dissolved in 1 ml 7 M HCl + 0.001% H_2O_2 was loaded on each column, and eluted with 2 M HCl + 0.001% H_2O_2.

In the case of the "fast" column, 30 elution cuts of varying volumes were collected in 15-ml centrifuge tubes. Twenty-five cuts were collected from the "slow" column. All cuts were diluted with 18 M-Ohm DI H_2O to a volume of 1 ml, and saved for measurement of Fe concentration and isotopic composition.

4.4. UV–VIS analysis (Fe concentration)

Prior to isotope ratio measurement, the Fe concentration of timed aliquots and column cuts was confirmed by UV–VIS analysis (To et al., 1999). Approximately 20% of each aliquot was used for this analysis. Measurements were performed using a diode array spectrophotometer (Shimadzu UV1601-PC), and Fe concentrations determined by linear regression relative to a calibration curve defined by four standards of known Fe concentration and a blank. Using this method, the concentration of Fe was routinely determined to $\pm 5\%$ ($\pm 2\sigma$).

Once Fe concentration was determined, the remainder of the aliquots from the equilibrium experiments and the eluted cuts from the column experiments were prepared for isotopic analysis. The samples were reduced to almost dryness and reconstituted in 0.05 M HNO_3 to a final Fe concentration of 3–4 ppm. Further dilutions with 0.05 M HNO_3 were made according to instrument running conditions for the particular day.

4.5. MC-ICP-MS analysis (isotopic composition)

4.5.1. Data acquisition

All Fe isotope ratios were measured by MC-ICP-MS (VG Elemental Plasma54) at the University of Rochester. The Plasma54 is a double-focusing magnetic sector mass spectrometer with one fixed axial Faraday collector and eight moveable Faraday collectors, four on either side of the central axial collector (Walder and Freedman, 1992).

Isobaric interferences at masses 54 and 56 from ArN^+ and ArO^+ present a challenge when measuring

Fe isotope ratios. These interferences arise from the Ar gas used to generate the plasma and from N and O present both in the atmosphere and in the solution. The accuracy and precision of the Fe isotope ratio measurements by MC-ICP-MS are limited by our ability to minimize and correct for these interferences.

To help minimize the contributions from ArN^+ and ArO^+, a desolvation system (Cetac Aridus I) is utilized, operated without the N_2 gas input (Belshaw et al., 2000). Using the desolvation system in this way reduces the ArN^+ signal to <2.7 mV and the ArO^+ to <5 mV. The use of HCl rather than HNO_3 as the solvent for samples was found to have minimal impact on the ArN^+ signal; presumably, substantial N is obtained from impurity in the Ar gas supply.

In practice, ArN^+ and ArO^+ intensities are stable to better than $\pm 5\%$ over several hours for any given plasma tuning conditions (Anbar et al., 2000). Therefore, the instrument is tuned on Cu and the intensities of the ArN^+ and ArO^+ ion beams are monitored and stored as external variables prior to introduction of Fe into the system. These externally stored ArN^+ and ArO^+ intensities are used to correct the mass 54 and 56 signals during all subsequent standard and sample runs.

To reduce the significance of these residual ArO^+ and ArN^+ interferences relative to the samples, Fe is run close to the maximum possible intensity (i.e., 8–10 V on ^{56}Fe) by adjusting the concentrations of the sample solutions. Under these conditions, the contribution of ArO^+ to the mass 56 signal is $<1‰$, and the contribution of ArN^+ to the mass 54 signal is $<6‰$. By closely matching the concentrations of the standard and the sample solutions, the effects of deficiencies in the corrections of ArO^+ and ArN^+ interferences are minimized in the determination of $\delta^{56}Fe$ and $\delta^{57}Fe$ (Belshaw et al., 2000).

As a quality control on our sample measurements, measurements of the gravimetric Fe standard are interspersed with the JMC-Fe standard and the samples during the run.

4.5.2. Mass bias compensation

Substantial instrumental mass bias in ICP-MS analyses results from the more efficient transmission of heavy, as opposed to light ions from the ion source to the mass analyzer. Consequently, the measured isotope ratios deviate from the actual ratios by 1–2% amu^{-1} in favor of heavier isotopes (Russ and Bazan, 1987). Without some method to compensate for this effect and its variability with time and sample matrix, precise measurements of isotopic differences are not possible.

Commonly, a "mass bias factor" (f) is used in an attempt to correct for mass bias. To determine f in ICP-MS, an element of known isotopic composition close in mass to the element of interest is added to samples and standards as an internal reference (Longerich et al., 1987). The measured, unknown isotope ratios can then be corrected for mass bias by applying either the empirically derived exponential or power laws (Hart and Zindler, 1989). When using Cu to correct for mass bias of Fe, the exponential law leads to the following relationship:

$$\left(^{56}Fe/^{54}Fe\right)_t = \left(^{56}Fe/^{54}Fe\right)_m \left(^{56}M/^{54}M\right)^f \quad (1)$$

and

$$f = \ln\left[\left(^{63}Cu/^{65}Cu\right)_t/\left(^{63}Cu/^{65}Cu\right)_m\right]/\ln\left(^{63}M/^{65}M\right) \quad (2)$$

where t and m denote the true and measured isotope ratios, and M are the atomic weights of the isotopes. A similar expression can be obtained for the power law.

This approach requires that the analyte and "spike" elements follow the same fractionation behavior; i.e., $f_{Fe}=f_{Cu}$. However, this is apparently not the case at high precision for Cu and Zn (Maréchal et al., 1999), Pb and Tl (White et al., 2000) and Mo, Zr and Ru (Anbar et al., 2001), which can lead to analytical error. Therefore, we explored this assumption for Fe and Cu.

We selected Cu as our elemental spike for Fe isotope measurements because it is similar in mass to Fe and there are no isobaric interferences between Cu and Fe. The JMC-ICP Cu solution was added to each Fe sample and standard so that the concentration of Cu was equal to the concentration of Fe.

A plot of $\ln(^{56}Fe/^{54}Fe)_m$ vs. $\ln(^{63}Cu/^{65}Cu)_m$ can be used to determine the validity of the assumption that $f_{Fe}=f_{Cu}$, by comparing the observed and expected slopes; the expected slopes are purely a function of atomic masses (Maréchal et al., 1999; Anbar et al., 2001). Fig. 3 illustrates the relationship of the slopes of

the JMC-Fe standard and our Grav-Fe standard from a typical run to the values predicted by the exponential and power laws. These slopes deviate from the exponential and power law predictions. Hence, as with other element pairs, it appears that $f_{Fe} \neq f_{Cu}$ to arbitrarily high precision. The deviation of the data from either law varies from day to day. However, the fractionation behavior is constant for any given run (i.e., $f_{Fe}/f_{Cu} \sim$ constant), as demonstrated by the linear correlations seen in Fig. 3. Therefore, it is possible to apply a regression method to determine δ^{56}Fe and δ^{57}Fe, as detailed elsewhere (Maréchal et al., 1999; White et al., 2000; Anbar et al., 2001). Briefly, this method takes advantage of the observation that samples with different true Fe isotopic compositions plotted, as in Fig. 3, lie along parallel lines with different intercepts. Consequently, δ^{56}Fe and δ^{57}Fe of a sample can be determined from the offset along the ln(^{56}Fe/^{54}Fe) axis between the sample data and the regression line defined by the JMC-Fe standard.

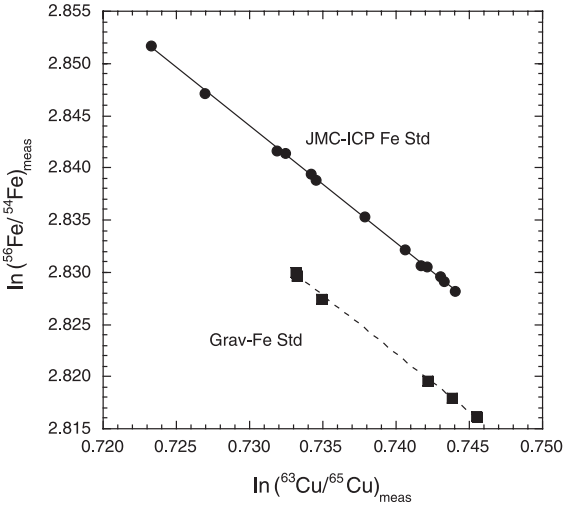

Fig. 3. ln(^{56}Fe/^{54}Fe)$_{measured}$ vs. ln(^{63}Cu/^{64}Cu)$_{measured}$ of JMC-Fe and Grav-Fe from a typical session. The offset between the trends of the two standards reflects the true difference in isotopic composition between these materials, $\sim$ 10.9‰. The slopes from the JMC-Fe Standard and Grav Fe Standard data are -1.12 ($R^2 = 0.9995$) and -1.11 ($R^2 = 0.9987$), respectively. Neither slope matches that predicted from the power law (-1.004) or the exponential law (-1.16). This indicates that $f_{Fe} \neq f_{Cu}$. However, the linearity of these trends shows that $f_{Fe}/f_{Cu} \sim$ constant for an entire day's session, permitting precise determination of δ^{56}Fe (see text).

The range of mass measurable on the Plasma54 at the atomic mass of Fe is only 4–5 amu. The mass spread for measuring Fe and Cu isotopes (54 to 65) is $\sim$ 11 amu. Consequently, two measurement cycles are required to measure both Fe and Cu isotopes. The use of two measurement cycles results in a slight loss of precision compared to that achievable by static measurement. For each sample or standard measurement, one block of six ratios is measured.

4.5.3. Data integrity

Two procedures are routinely followed to verify the integrity of our δ^{56}Fe determinations. First, the measured δ^{56}Fe of the Grav-Fe standard is compared to the known value (-10.9‰). Over a period of $\sim$9 months and $\sim$ 75 individual analyses, we have reproduced the known value with an external precision of better than ± 0.4‰ ($\pm 2\sigma$). This is comparable to the precision obtained with an earlier standard, reported in Anbar et al. (2000).

Second, to verify that the ArO^+ and ArN^+ interferences are properly corrected, both δ^{56}Fe and δ^{57}Fe are determined and compared for all the samples and JMC-Fe standards run in each analytical session. If the measured δ^{56}Fe and δ^{57}Fe result from mass-dependent fractionation, then a plot of δ^{56}Fe vs. δ^{57}Fe will have a slope of $\sim$ 0.68 (Criss, 1999). Uncorrected isobaric interferences or non-mass-dependent contributions (e.g., contamination from Grav-Fe) would produce deviations from this slope. This is illustrated in Fig. 4, which plots δ^{57}Fe vs. δ^{56}Fe from a typical experiment. The slope is $\sim$ 0.66, in good agreement with the expected value.

Data quality is quite sensitive to errors in the corrections for ArO^+ and ArN^+. The consequences of such errors can be minimized by carefully matching the concentrations of samples and standards (Belshaw et al., 2000). However, poorly matched sample/standard pairs result in degraded statistics, and performance may vary considerably between analytical sessions because of suboptimal tuning of the desolvator and variability in the quality of sample-standard matching. The importance of these problems is magnified when poorly understood changes in the plasma source lead to instability in the ion beam. Therefore, we have found it critical to analyze the Grav-Fe standard alongside samples and the JMC-Fe standard as a quality control measure. Based on analyses of the

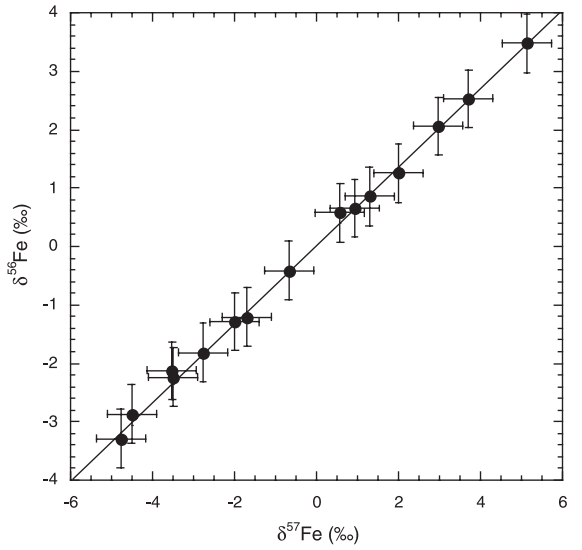

Fig. 4. δ^{56}Fe vs. δ^{57}Fe of samples for a typical experiment. Uncertainties are $\pm 2\sigma$. The solid line represents the theoretical relationship between δ^{56}Fe and δ^{57}Fe, assuming mass-dependent fractionation.

Grav-Fe standard conducted concurrently with samples, a precision of ± 0.3 ‰ ($\pm 2\sigma$) was obtained when analyzing fractionations in aliquots from the equilibration rate experiments. However, for the rate-dependent elution experiments, somewhat degraded precision of $\sim \pm 0.5$ ‰ ($\pm 2\sigma$) was obtained.

5. Results and discussion

5.1. Equilibration rate experiments

The equilibration rate experiments demonstrate that dissolved and resin-bound Fe are almost completely equilibrated in our batch experiments within $\sim$ 1 min.

This is first seen, crudely, in experiment #1. Constraints can be placed on the rate of equilibration from the observed changes in total Fe concentration of the timed aliquots; equilibrium between the Fe on the resin and in solution is reached when the dissolved Fe concentration no longer changes. Fig. 5 shows the Fe concentration of the timed aliquots during desorption from the resin. The equilibrium concentration in solution is $\sim$ 22.5 ppm, based on the identical concentration measurements at 8 and 24 h. This compares favorably with the expected concentration of $\sim$ 21.8 ppm predicted from the known K_D (Table 2). It is apparent that the dissolved concentration at 1 min (21.6 ± 1.1 ppm) is statistically indistinguishable from the equilibrium value. Given our analytical uncertainties, this indicates that at least 91% of the adsorbed Fe has equilibrated with the new solution composition within 1 min.

A more refined estimate of equilibration rate is obtained from experiment #2. When the equilibrated ^{54}Fe spike solution (δ^{56}Fe = – 998 ‰) is replaced with the JMC-Fe standard solution (δ^{56}Fe = 0 ‰) at the same Fe concentration, the bulk Fe concentrations on the resin and in solution were maintained at equilibrium values. However, the isotopic compositions of these reservoirs were suddenly out of equilibrium. Hence, the isotopic composition of dissolved Fe must shift as isotopes exchange between resin and solution to attain isotopic equilibrium. In such an experiment, precise measurement of δ^{56}Fe of dissolved Fe in each timed aliquot can be used to obtain a precise assessment of the extent of isotopic equilibrium at each time. By definition, once δ^{56}Fe of the resin and solution reservoirs are identical, 100% equilibration has been achieved.

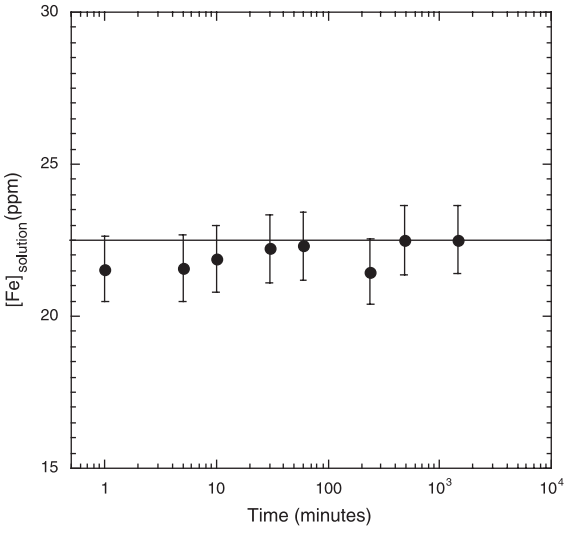

Fig. 5. Measured [Fe] vs. time in equilibration rate experiment #1. The horizontal line denotes the equilibrium value, as indicated by the data at 8 and 24 h. By 1 min, [Fe] is 21.6 ± 1.1 ppm ($\pm 2\sigma$), statistically indistinguishable from [Fe] at equilibrium (22.5 ppm).

At $t=12$ h, the δ^{56}Fe on the resin and in solution were identical (-808.5 ‰), demonstrating that complete equilibration was achieved by this time. Approach to this equilibrium is apparently very rapid (Fig. 6); the solution composition shifts from an initial value of 0 ‰ to -806.2 ‰, -807.3 ‰ and -808.2 ‰ at $t=1$, 5 and 10 min, respectively. δ^{56}Fe of the solution is within error of the equilibrium value after ~ 10 min.

We can use these data to estimate the extent of equilibration between dissolved and resin-bound Fe vs. time. From δ^{56}Fe of dissolved Fe at $t=0$ (δ^{56}Fe = 0 ‰) and $t=12$ h (δ^{56}Fe = -808.5 ‰), holding the concentration of total Fe constant, we can determine the net quantity of ^{54}Fe that must be transferred from resin (δ^{56}Fe = -998 ‰ at $t=0$) to solution to obtain the equilibrium isotopic composition. δ^{56}Fe of dissolved Fe at any intermediate time t can then be used to determine the fraction of this quantity (F) that has transferred by time t. Hence, δ^{56}Fe at 1, 5, and 10 min correspond to $F=98.8\%$, 99.4% and 99.8%, respectively (Fig. 7). These results demonstrate that equilibration between dissolved and resin-bound Fe is rapid.

It is clear from this experiment that experiments conducted on timescales as short as 1 min should be dominated by equilibrium conditions. These findings are consistent with the interpretation of Anbar et al. (2000). Much slower equilibration rates have been reported in similar batch experiments (Skulan et al., 2000; Beard et al., 2000). Although the full experimental details of these studies have not yet been published, they differed from our experiments in the use of microporous rather than macroporous resin. This difference would be expected to result in faster equilibration rates in our studies.

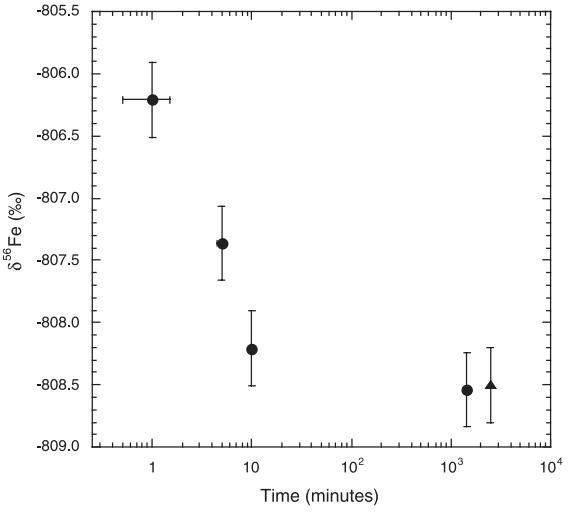

Fig. 6. δ^{56}Fe of the solution aliquots (●) vs. time in equilibration rate experiment #2. δ^{56}Fe of resin-bound Fe at 12 h (▲) has been offset from this time for clarity. δ^{56}Fe at $t=10$ min is within error of δ^{56}Fe of the resin value (-808.5 ‰).

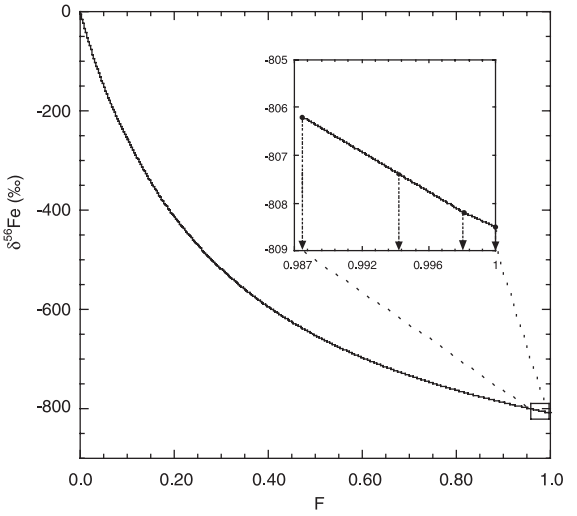

Fig. 7. Modeled δ^{56}Fe of dissolved Fe vs. F, to describe equilibration rate experiment #2. F is a measure of the extent of equilibration (see text). At $t=0$, $F=0$ and δ^{56}Fe = 0 ‰. As F increases, there is net transfer of ^{54}Fe from the resin (with initial δ^{56}Fe = -998 ‰) to solution. When $F=1$, δ^{56}Fe of dissolved and resin-bound Fe are identical (-808.5 ‰). Data all fall in the region $806\text{ ‰} < \delta^{56}\text{Fe} \leq 808.5\text{ ‰}$ (inset), which corresponds to $F>0.987$. Arrows indicate the values of F corresponding to each δ^{56}Fe measurement.

The δ^{56}Fe measurements in experiment #1 can be used to place an upper limit on $^{54}K_D/^{56}K_D$ in a single batch equilibration. δ^{56}Fe for all of the timed aliquots of the solution and for the resin over a period of 24 h are shown in Fig. 8. δ^{56}Fe for all but one of the solution aliquots are statistically indistinguishable from 0 ‰. In addition, δ^{56}Fe all of the solution aliquots are indistinguishable from the isotopic composition of resin-bound Fe sampled after 24 h. The maximum possible difference between the mean δ^{56}Fe of the solution aliquots and δ^{56}Fe of the resin-bound Fe at equilibrium is ~ 1 ‰ at 95%

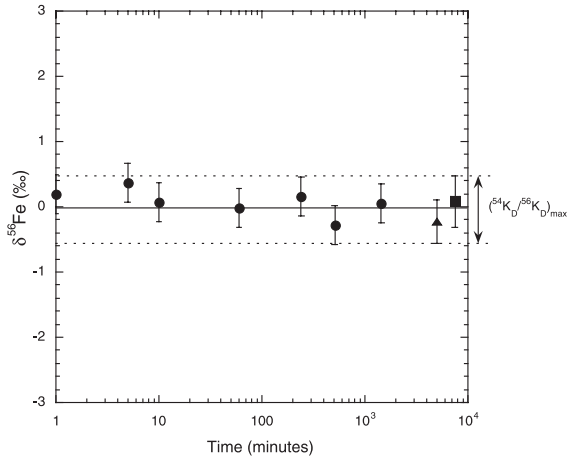

Fig. 8. δ^{56}Fe vs. time in equilibration rate experiment #1. δ^{56}Fe of the solution aliquots at time t (●). δ^{56}Fe of resin-bound Fe after 24 h (▲) and the mean δ^{56}Fe of all the solution aliquots (■) are offset for clarity. δ^{56}Fe of all of the solution aliquots are within error of the value for resin-bound Fe. The maximum possible difference between δ^{56}Fe of the Fe on the resin and dissolved Fe, indicated by the arrow between the dotted lines, is ~ 1 ‰ at 95% confidence. Hence, $^{54}K_D/^{56}K_D < 1.001$.

confidence. This translates to $^{54}K_D/^{56}K_D < 1.001$. This finding is consistent with Anbar et al.'s (2000) inference from chromatographic experiments of a single-step fractionation factor of order 1.0001; such a small fractionation factor should be undetectable in the present experiment, given the limits of analytical precision. Successive batch experiments couldproduce a more accurate determination of $^{54}K_D/^{56}K_D$. However, the number of theoretical plates in the chromatrographic experiments approaches 100. Hence, to have sufficient amounts of Fe at the end of such a series for precise δ^{56}Fe measurements, impractically large quantities of acid and resin would be necessary. A much smaller number of batch experiments could be useful if the fractionation approaches the upper range of $^{54}K_D/^{56}K_D$ estimates.

5.2. Rate dependence experiments

Although the equilibration rate experiments demonstrate rapid equilibration, they do not entirely preclude the possibility of kinetic effects in a chromatographic system because the timescale available for equilibration between resin and solution at each theoretical plate is significantly shorter than the timescale of these experiments. However, elution experiments at different rates are revealing.

Comparison of the elution bands of the two columns confirms that flow rate affects the interactions between dissolved Fe and the resin. This is clearly seen by comparing the elution curves of the two columns (Fig. 9). The elution band of the fast column is much broader and less symmetric than the sharper band of the slow column, which suggests that nonequilibrium processes are more important at the higher elution rate. This difference was visually apparent during the experiment itself: During elution from the fast column, a yellow Fe band initially visible at the top of the column became diffuse as it progressed down. In contrast, the Fe band remained sharp and distinct throughout elution from the slow column. Presumably, this reflects the lesser time available to attain "local equilibrium" during elution at the higher rate. This time can be estimated from the number of theoretical plates in the column and the flow rate through the column. The number of theoretical plates was determined from each elution curve (Skoog and Leary, 1992). The contact time at each plate was found to be ~ 1 and ~ 5 s for the fast and slow columns, respectively. By comparison, the time constant for equilibration, which can be estimated

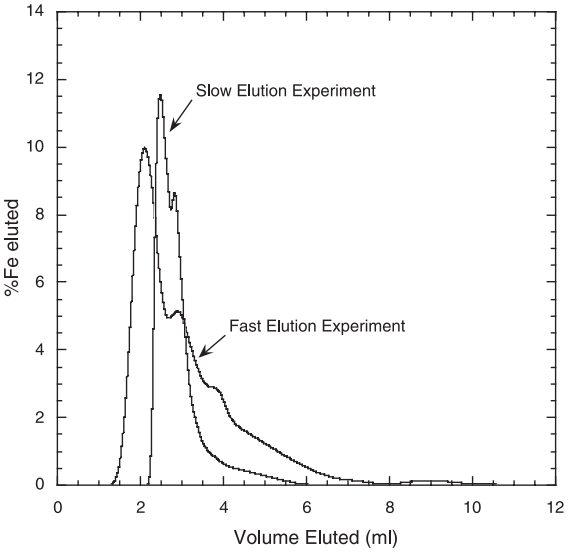

Fig. 9. Fe elution curves for the fast and slow elution experiments.

from either of the equilibration experiments, is of order 10 s. Thus, while neither column is likely to represent an ideal equilibrium case, the slow column should be significantly closer to this case than the fast column.

The fractionation of Fe isotopes by these two columns was similarly distinct. This is most readily illustrated by plotting δ^{56}Fe of each elution fraction against the cumulative percent of recovered Fe (Fig. 10). This abscissa facilitates comparison of the two experiments because the different elution curves make it impractical to ensure identical fractional recovery of Fe in most collected elution fractions. It is clear from such a comparison that the extent of fractionation is substantially larger in the slow column—a range of ~ 5.5 ‰ is observed in this experiment, compared to only ~ 2 ‰ in the elution fractions from the fast column. This difference is also reflected in the slopes of lines defined by the two experiments, which differ by a factor of ~ 2.

As observed by Anbar et al. (2000), ^{56}Fe elutes more rapidly than ^{54}Fe, consistent with the hypothesis that $^{54}K_D/^{56}K_D>1$.

The difference in fractionation behavior in these two experiments demonstrates that Fe isotope fractionation in this system is sensitive to reaction rate. However, the observation that the magnitude of fractionation increases as elution rate decreases demonstrates that *the magnitude of Fe isotope fractionation increases as equilibrium is approached.* This is extremely strong evidence for the existence of an equilibrium isotope effect.

At the same time, these findings demonstrate that kinetic complications must be considered when deriving equilibrium fractionation factors from chromatographic data to better than order-of-magnitude accuracy. For this reason, Anbar et al.'s (2000) inference from a relatively rapid chromatographic experiment that $^{54}K_D/^{56}K_D \sim 1.0001$ is best regarded as a lower limit.

5.3. Fractionation mechanism

Based on these findings, the fractionation of Fe isotopes during anion exchange chromatography in HCl can be used to infer the existence of an equilibrium isotope effect. It is likely that this effect stems from isotope effects during equilibrium speciation of Fe aquo–chloro complexes. This relevant equilibrium constant(s) can be identified by considering the definition of K_D for Fe in this system:

$$K_D = \frac{[R-FeCl_4]}{[Fe(H_2O)_6^{3+}] + [FeCl(H_2O)_5^{2+}] + [FeCl_2(H_2O)_4^{+}] + [FeCl_3(H_2O)_3^{0}] + [FeCl_4^{-}]}$$

Substituting the equilibrium expressions of the reactions in Table 1, it can be shown that:

$$\frac{^{54}K_D}{^{56}K_D} = \frac{^{54}K_1\,^{54}K_2\,^{54}K_3\,^{54}K_4\,^{54}K_R}{^{56}K_1\,^{56}K_2\,^{56}K_3\,^{56}K_4\,^{56}K_R} \times \frac{(1+{}^{56}K_1[Cl^-]+{}^{56}K_1\,^{56}K_2[Cl^-]^2+\,{}^{56}K_1\,^{56}K_2\,^{56}K_3[Cl^-]^3+\,{}^{56}K_1\,^{56}K_2\,^{56}K_3\,^{56}K_4[Cl^-]^4)}{(1+\,{}^{54}K_1[Cl^-]+\,{}^{54}K_1\,^{54}K_2[Cl^-]^2+\,{}^{54}K_1\,^{54}K_2\,^{54}K_3[Cl^-]^3+\,{}^{54}K_1\,^{54}K_2\,^{54}K_3\,^{54}K_4[Cl^-]^4)}$$

In 2 M HCl, using the equilibrium constants in Table 1, this expression can be simplified to a first approximation as follows:

$$\frac{^{54}K_D}{^{56}K_D} \sim \frac{^{54}K_1^{54}K_2^{54}K_3^{54}K_4^{54}K_R}{^{56}K_1^{56}K_2^{56}K_3^{56}K_4^{56}K_R} \times \frac{^{56}K_1^{56}K_2[Cl^-]^2}{^{54}K_1^{54}K_2[Cl^-]^2} \sim \frac{^{54}K_3^{54}K_4^{54}K_R}{^{56}K_3^{56}K_4^{56}K_R}$$

Hence, to first order, the isotope separation is governed by equilibria between R-$FeCl_4$ and $FeCl_4^-$, $FeCl_4^-$ and $FeCl_3(H_2O)_3^\circ$, and between $FeCl_3(H_2O)_3^\circ$ and $FeCl_2(H_2O)_4^+$.

It is well known that isotope fractionation at equilibrium between two chemical compounds can be driven by changes in the bonding environment of the central atom (Bigeleisen and Mayer, 1947). Since the Fe coordination environments of $FeCl_4^-$ and R-$FeCl_4$ are identical, it is unlikely that fractionation occurs during the binding of $FeCl_4^-$ to the resin. In this case, $^{54}K_R/^{56}K_R = 1$, and $^{54}K_D/^{56}K_D \sim {}^{54}K_3/^{56}K_3 \times {}^{54}K_4/^{56}K_4$. However, there is a large difference in coordination

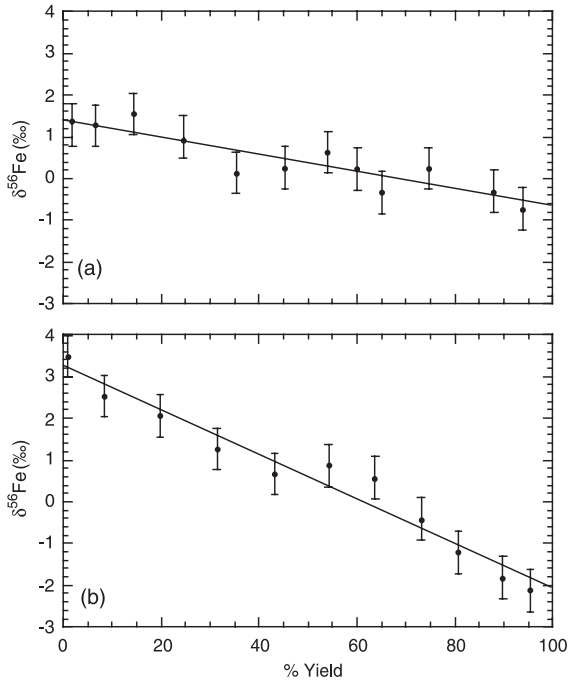

Fig. 10. δ^{56}Fe vs. % yield for both the fast (a) and slow elution (b) experiments. In the fast elution experiment, a smaller fractionation is observed at each step in the elution. The slope of the fast elution experiment is smaller (-0.02, $R^2=0.8529$) than that of the slow elution experiment (-0.05, $R^2=0.9573$), and a much smaller range of δ^{56}Fe values is observed in the fast elution experiment (~ 2‰) than in the slow experiment (~ 5.5‰). In each experiment, $\sim 100\%$ of the Fe loaded was recovered, and $\delta^{56}\text{Fe} \sim 0$ when integrated over all elution fractions as required by mass balance.

environment between $^{54}FeCl_4^-$ and $FeCl_2(H_2O)_4^+$; the former is tetrahedral, while the latter is octahedral, as are $Fe(H_2O)_6^{3+}$and $FeCl(H_2O)_5^{2+}$ (Magini and Radnai, 1979; Bjerrum and Lukes, 1986). The geometry of $FeCl_3(H_2O)_3^\circ$, a matter of some dispute. It may be octahedral or trigonal bipyramidal but is clearly not tetrahedral (Magini and Radnai, 1979; Apted et al., 1985). Hence, isotope fractionation between $FeCl_4^-$ and Fe aquo–cloro complexes is not surprising, and is consistent with theoretical predictions (Schauble et al., in press). Moreover, bonds between Fe^{3+} and H_2O are moderately stronger than between $Fe^{3+}$and Cl^- (Schauble et al., in press), as can be seen from the shorter length of Fe–O vs. Fe–Cl bonds in complexes of similar geometry (Hair and Beattie, 1977). Therefore, it is not surprising that this fractionation would favor preferential partitioning of the lighter isotope, ^{54}Fe, into $FeCl_4^-$ and R-$FeCl_4$. Hence, both the existence and direction of the observed fractionation are consistent with our understanding of Fe speciation.

This is not a novel type of hypothesis to account for isotope fractionation in ion exchange systems. For example, a similar hypothesis has been used to explain the separation of B isotopes during anion exchange chromatography (Kakihana et al., 1977). In this system, separation of ^{10}B from ^{11}B is attributed to an equilibrium fractionation between tetrahedrally coordinated $B(OH)_4^-$, which adsorbs to the resin, and the trigonal planar $B(OH)_3$ species, which remains in solution. In this case, the lighter ^{10}B isotope is enriched in the resin phase whereas the heavier ^{11}B isotope is enriched in the solution. This observation is consistent with the shorter B–O bond lengths (and hence stronger B bonding environment) in the trigonal species.

To account for the rate dependence of fractionation during elution, we suggest that the rate of equilibration is diffusion-limited. During rapid elution, there is less time for dissolved Fe complexes to diffuse into the deeper macro and micropores of the resin. Because binding of $FeCl_4^-$ to the resin is necessary to separate $FeCl_4^-$ from other, isotopically fractionated Fe–Cl complexes, slow diffusion limits the extent of isotope separation compared to the ideal case. It is important to stress that the hypothesis does not require that ^{54}Fe and ^{56}Fe diffuse at different rates. Slow diffusion at identical rates could result in an under-expression of an equilibrium isotope effect, just as observed.

6. Conclusions

Based on our findings, isotope fractionation during elution of Fe from columns packed with macroporous anion exchange resin results from an equilibrium Fe isotope effect. Approach to this equilibrium is very rapid, but may not be fast enough to overcome kinetic complications during rapid elution. Such complications, perhaps related to diffusion, reduce the extent of isotope separation achieved during chromatography because they inhibit equilibration at each "theoretical plate" comprising the ion exchange column.

In light of these findings, it is imperative to obtain $\sim 100\%$ yield from the separation chemistry to pro-

vide confidence that the observed isotopic fractionation originates from the sample itself rather than the chemical process performed on the sample.

In addition, these findings underscore the warnings of Anbar et al. (2000): that simple nonbiological chemical processes can fractionate Fe isotopes; that Fe isotope fractionation may occur during equilibrium processes; and that equilibrium fractionation effects during speciation of dissolved Fe complexes are probably important in nature.

Indeed, these warnings must be considered all the more seriously because the present results imply that the magnitude of the equilibrium fractionation factor estimated previously is too low. Based on the arguments presented above, combined with the findings of Anbar et al. (2000), $1.0001 < {}^{54}K_D/{}^{56}K_D < 1.001$. Therefore, it is possible that simple equilibrium isotope effects could give rise to natural δ^{56}Fe variations of 1‰ magnitude even in very simple reactions. This conclusion is consistent with the ferrihydrite precipitation experiments of Bullen et al. (in press) and the theoretical study of Schauble et al. (in press). Hence, δ^{56}Fe data cannot be unambiguously interpreted as biosignatures until nonbiological fractionation effects in nature are more thoroughly understood.

Acknowledgements

We thank T. Gennett, P. Holland, W. Saunders, and J. McGarrah for discussions. This research was supported by grants from NSF-LExEn (CHE-9714282) and the NASA Astrobiology Institute (ADA). **[EO]**

References

Anbar, A.D., Roe, J.E., Barling, J., Nealson, K.H., 2000. Nonbiological fractionation of iron isotopes. Science 288, 126–128.

Anbar, A.D., Knab, K., Barling, J., 2001. Precise determination of variation in the isotopic composition of molybdenum using MC-ICP-MS. Anal. Chem. 73, 1425–1431.

Apted, M.J., Waychunas, G.A., Brown, G.E., 1985. Structure and specification of iron complexes in aqueous solutions determined by X-ray absorption spectroscopy. Geochim. Cosmochim. Acta 49, 2081–2089.

Beard, B.L., Johnson, C.M., Cox, L., Sun, H., Nealson, K.H., Aguilar, C., 1999. Iron isotope biosignatures. Science 285, 1889–1892.

Beard, B.L., Johnson, C.M., Skulan, J.L., O'Leary, J., Sun, H., 2000. Fe isotope fractionation in nature: when is it bugs, when is it not? EOS Trans. AGU 81, F195.

Belshaw, N.S., Zhu, Y.G., Nions, R.K., 2000. High precision measurement of iron isotopes by plasma source mass spectrometry. Int. J. Mass Spectrom. 197, 191–195.

Bigeleisen, J., Mayer, M.G., 1947. Calculation of equilibrium constants for isotopic exchange reactions. J. Chem. Phys. 15 (5), 261–267.

Bjerrum, J., Lukes, I., 1986. The iron–chloride system. A study of the stability constants and of the distribution of the tetrachloro species between organic solvents and aqueous chloride solutions. Acta Chem. Scand., Ser. A 40, 31–40.

Brantley, S.L., Liermann, L., Bullen, T.D., 2001. Fractionation of Fe isotopes by soil microbes and organic acids. Geology 29 (6), 535–538.

Bullen, T.D., White, A.F., Childs, C.W., Vivit, D.V., Schultz, M.S., 2001. Demonstration of significant abiotic iron isotope fractionation in nature. Geology 29 (8), 699–702.

Connick, R.R., Coppel, C.P., 1959. Kinetics of the formation of the ferric chloride complex. J. Am. Chem. Soc. 81, 6389–6394.

Criss, R.E., 1999. Principles of Stable Isotope Distribution. Oxford Univ. Press, New York.

Gluekauf, E., 1955. Theory of chromatography: Part 9. The "theoretical plate" concept in column separations. Trans. Faraday Soc. 51, 34–44.

Gluekauf, E., 1958. Theory of chromatography: Part 11. Enrichment of isotopes by chromatography. Trans. Faraday Soc. 54, 1203–1205.

Hair, N.J., Beattie, J.K., 1977. Structure of hexaaquairon (III) nitrate trihydrate. Comparison of iron (II) and iron (III) bond lengths in high-spin octahedral environments. Inorg. Chem. 16, 245–250.

Halliday, A.N., Lee, D., Christensen, J.N., Walder, A.J., Freedman, P.A., Jones, C.E., Hall, C.M., Yi, W., Teagle, D., 1995. Recent developments in inductively-coupled plasma magnetic-sector multiple collector mass-spectrometry. Int. J. Mass Spectrom. Ion Process. 146, 21–33.

Harris, D.C., 1991. Quantitative Chemical Analysis, 3rd ed. Freeman, New York, NY.

Hart, S.R., Zindler, A., 1989. Isotope fractionation laws: a test using calcium. Int. J. Mass Spectrom. Ion Process. 89, 287–301.

Helfferich, F., 1995. Ion Exchange. Dover Publications, New York.

Hoefs, J., 1989. Stable Isotope Geochemistry, 3rd ed. Springer-Verlag, New York.

Kakihana, H., Kotaka, M., Satoh, S., Nomura, M., Okamoto, M., 1977. Fundamental studies on the ion-exchange separation of boron isotopes. Bull. Chem. Soc. Jpn. 50, 158–163.

Longerich, H.P., Fryer, B.J., Strong, D.F., 1987. Determination of lead isotope ratios by inductively coupled plasma-mass spectrometry (ICP-MS). Spectrochim. Acta, B 42, 39–48.

Machlan, L.A., Gramlich, J.W., 1988. Isotopic fractionation of gallium on an ion-exchange column. Anal. Chem. 60, 37–39.

Magini, M., Radnai, T., 1979. X-ray diffraction study of ferric chloride solutions and hydrated melt. Analysis of the iron (III)–chloride complexes formation. J. Chem. Phys. 71, 4255–4262.

Maréchal, C.N., Télouk, P., Albarède, F., 1999. Precise analysis of copper and zinc isotopic compositions by plasma-source mass spectrometry. Chem. Geol. 156, 251–273.

Marhol, M., 1982. Ion exchangers in analytical chemistry. Their properties and use in inorganic chemistry. In: Svehal, G. (Ed.), Wilson and Wilson's Comprehensive Analytical Chemistry, vol. XIV. Elsevier, New York, pp. 21–51.

Martin, A.J.P., Synge, R.L.M., 1941. A new form of chromatogram employing two liquid phases: 1. A theory of chromatography: 2. Application to the micro-determination of the higher monoamino-acids in proteins. Biochem. J. 35, 1358–1368.

Rehkamper, M., Halliday, A.N., 1999. The precise measurement of Tl isotopic compositions by MC-ICP-MS: application to the analysis of geological materials and meteorites. Geochim. Cosmochim. Acta 63, 935–944.

Russ III, G.P., Bazan, J.M., 1987. Isotopic ratio measurements with an inductively coupled plasma source mass spectrometer. Spectrochim. Acta, B 42, 49–62.

Russell, W.A., Papanastassiou, D.A., 1978. Calcium isotope fractionation in ion-exchange chromatrography. Anal. Chem. 50 (8), 1151–1154.

Russell, W.A., Papanastassiou, D.A., Tombrello, T.A., 1978. Ca isotope fractionation on the Earth and other solar system materials. Geochim. Cosmochim. Acta 42, 1075–1090.

Schauble, E.A., Rossman, G.R., Taylor, H.P., 2001. Theoretical estimates of equilibrium Fe-isotope fractionations from vibrational spectroscopy. Geochim. Cosmochim. Acta 65, 2487–2597.

Schwarz, H.A., Dodson, R.W., 1976. Kinetic of dissociation of ferric chloride complexes. Stability constants of inner- and outer-sphere complexes. J. Phys. Chem. 80, 2801–2804.

Skoog, D.A., Leary, J.J., 1992. Principles of Instrumental Analysis, 4th ed. Saunders, Fort Worth.

Skulan, J.L., Sun, H., Beard, B.L., O'Leary, J., Johnson, C.M., Nealson, K.H., Cox, L., 2000. Progress in the development of an iron isotope biosignature. EOS Trans. AGU 81, S30.

Strahm, U., Patel, R.C., Matljevic', E., 1979. Thermodynamics and kinetics of aqueous iron (III) chloride complexes formation. J. Phys. Chem. 83, 1689–1695.

Taylor, T.I., Urey, H.C., 1938. Fractionation of the lithium and potassium isotopes by chemical exchange with zeolites. J. Chem. Phys. 6, 429–438.

To, T.B., Nordstrom, D.K., Cunningham, K.M., Ball, J.W., McClesky, R.B., 1999. New method for the direct determination of dissolved Fe(III) concentration in acid mine waters. Environ. Sci. Technol. 33, 807–813.

Van der Walt, T.N., Strelow, F.W.E., Verjheij, R., 1985. The influence of crosslinkage on the distribution coefficients and anion exchange behaviour of some elements in hydrochloric acid. Solv. Extr. Ion Exch. 3, 723–740.

Walder, A.J., Freedman, P.A., 1992. Isotope ratio measurements using a double focusing magnetic sector mass analyser with an inductively coupled plasma ion source. J. Anal. At. Spectrom. 7, 571–575.

Walder, A.J., Platzner, A.I., Freedman, P.A., 1993. Isotope ratio measurements of lead, neodymium and neodymium–samarium, hafnium–lutetium mixtures with a double-focusing multiple collector mass spectrometer. J. Anal. At. Spectrom. 8, 19–23.

White, W.M., Albarède, F., Télouk, P., 2000. High-precision analysis of Pb isotope ratios by multi-collector ICP-MS. Chem. Geol. 167, 257–270.

Zhu, X.-K., O'Nions, R.K., Guo, Y., Reynolds, B.C., 2000a. Secular variation of iron isotopes in North Atlantic deep water. Science 287, 2000–2002.

Zhu, X.-K., O'Nions, R.K., Guo, Y., Belshaw, N.S., Rickard, D., 2000b. Determination of natural Cu-isotope variation by plasma-source mass spectrometry: implications for use as geochemical tracers. Chem. Geol. 163, 139–149.